Targeted small molecule identification using heartcutting liquid chromatography–infrared ion spectroscopy

Rianne E. van Outersterp[1], Jitse Oosterhout[1], Christoph R. Gebhardt[2], Giel Berden[1], Udo F.H. Engelke[3], Ron. A. Wevers[3], Filip Cuyckens[4], Jos Oomens[1,5], Jonathan Martens[1*]

[1]*Radboud University, Institute for Molecules and Materials, FELIX Laboratory, Toernooiveld 7, 6525 ED Nijmegen, The Netherlands.*
[2]*Bruker Daltonik GmbH & Co. KG, Fahrenheitstrasse 4, D-28359 Bremen, Germany*
[3]*Department of Laboratory Medicine, Translational Metabolic Laboratory, Radboud University Medical Center, 6525 GA Nijmegen, The Netherlands*
[4]*Drug Metabolism & Pharmacokinetics, Janssen R&D, Beerse, Belgium*
[5]*van't Hoff Institute for Molecular Sciences, University of Amsterdam, 1098XH Amsterdam, The Netherlands*
*corresponding author

KEYWORDS: infrared ion spectroscopy, heartcutting liquid chromatography, metabolomics, drug metabolism, pyridoxine-dependent epilepsy, diastereomers, midazolam

ABSTRACT: Infrared ion spectroscopy (IRIS) can be used to identify molecular structures detected in mass spectrometry (MS) experiments and has potential applications in a wide range of analytical fields. However, MS-based approaches are often combined with orthogonal separation techniques, in many cases liquid chromatography (LC). The direct coupling of LC and IRIS is challenging due to the mismatching timescales of the two technologies: an IRIS experiment typically takes several minutes, whereas an LC fraction typically elutes in less than a minute. To resolve this discrepancy, we present a heartcutting LC-IRIS approach using a setup consisting of two switching valves and two sample loops as an alternative to direct online LC-IRIS coupling. We show that this automated setup enables us to record multiple IR spectra for two LC-features from a single injection without degrading the LC-separation performance. We demonstrate the setup for application in drug metabolism research by recording six m/z-selective IR spectra for two drug metabolites from a single 2 µl sample of cell incubation extract. Additionally, we measure the IR spectra of two closely eluting diastereomeric biomarkers for the inborn error of metabolism pyridoxine dependent epilepsy (PDE-ALDH7A1), which shows that the heartcutting LC-IRIS setup has good sensitivity (requiring ~µl injections of ~µM samples) and that the separation between closely eluting isomers is maintained. We envision applications in a range of research fields, where the identification of molecular structures detected by LC-MS is required.

INTRODUCTION

Mass spectrometry (MS) is among the most popular analytical methods employed in a wide range of scientific fields, which can be attributed to its ultra-high sensitivity and selectivity as compared to alternative techniques, most notably nuclear magnetic resonance (NMR) spectroscopy. This allows for the detection of very low abundance analytes from complex mixtures, such as body fluids, containing thousands of molecular species. However, the amount of molecular structure information that can be extracted from an MS experiment is often limited. Each detected *m/z*-feature can potentially correspond to a number of structural isomers and determining which of these is actually present in a given sample is often nontrivial.[1-5] To address this, a range of orthogonal technologies hyphenated to MS have been developed, such as fragmentation technologies[6], ion mobility[7] and (liquid and gas) chromatography[8, 9].

Infrared ion spectroscopy (IRIS)[10-17] is a relatively novel approach integrating MS with infrared spectroscopy, so that an infrared spectrum, and hence direct information on chemical bonding, can be obtained for an isolated *m/z*-feature. Recent studies have detailed its potential for molecular structure elucidation in a variety of research fields including forensics[18-21], environmental science[22-24], drug development[25-27] and clinical research[25, 28, 29]. IRIS is an action spectroscopy technique; IR spectra are generated by recording the photodissociation of ions after irradiation at a series of IR laser frequencies. Plotting the extent of fragmentation as a function of the IR frequency provides the IR spectrum. IRIS can therefore be incorporated in an MS-based analytical workflow analogous to other fragmentation MS/MS methods. However, to record an entire IR spectrum, individual MS/MS spectra need to be recorded at each IR frequency of the laser (for example, 500-2000 cm^{-1} in 3-5 cm^{-1} steps), which typically involves the acquisition of 300-500 MS/MS spectra and all together requires >10 minutes. Previous work has shown that for experiments distinguishing between a few targeted "known unknowns", spectral libraries can be constructed that allow the distinction of compounds based on only a few isomer-specific wavelengths making the experiment much faster. However, more extensive IR spectra covering a broader frequency range are typically required for the identification of unknowns.

To avoid ionization suppression effects and to separate isomers, MS is often combined with an analytical separation technique in the analysis of complex biochemical samples. Liquid chromatography (LC) is the most widely used separation method, mainly due to its robustness and versatility in separating a wide variety of (non-volatile) chemical structures.[8, 30-32] However, the direct coupling of LC and IRIS is not trivial, due to the mismatching time-scales of the experiments; peak widths in state-of-the-art ultra-high pressure LC (UHPLC) separations are usually not longer than several seconds, much shorter than the ~10 min required for the acquisition of an IRIS spectrum. To address this challenge,

several approaches to LC-IRIS coupling have been proposed. Offline coupling involving fraction collection[27,33] provides the highest flexibility for both the LC- and IRIS-experiments, but has drawbacks in terms of potential sample loss, degradation and/or contamination, often giving an overall reduction in sensitivity. In contrast, online coupling gives the best potential for high-throughput methods, but puts severe limitations on either the resolution of the LC separation or the number of MS/MS spectra that can be acquired and thus the IR frequency range that can be covered.[25] As a third approach, a hybrid solution based on semi-online coupling via stop flow LC-IRIS has been demonstrated, although this also necessitates sacrifices in separation performance and sensitivity.[34]

Here, we demonstrate heartcutting LC-IRIS (analogous to heartcutting 2D-LC approaches) as an alternative approach. This involves an interface between the LC and MS systems consisting of two switching valves and two sample loops, comparable to the interface commonly used between the two LC-dimensions in 2D-LC systems[35-38]. With this setup, two fractions of eluent (containing separated *m/z* features of interest) from a single LC injection can be stored in sample loops and separately infused into the MS-instrument at reduced flow rates compared to those used for the LC separation. We demonstrate that this can provide ~20 minutes of stable ion signal, which allows for the acquisition of multiple IR spectra for each analyte.

EXPERIMENTAL

Chemicals

LC-MS grade water (H_2O) and methanol (MeOH) used for the LC separations were obtained from Biosolve (Valkenswaard, the Netherlands). LC-MS grade acetic acid (CH_3COOH) was obtained from Fisher Scientific (Geel, Belgium). Reference standards of phenylalanine (Phe), tryptophan (Trp) and caffeine (Caff) were obtained from Sigma-Aldrich (St. Louis, USA). Midazolam was purchased from Merck (Darmstadt, Germany). Acetonitrile (ACN) and formic acid (HCOOH) used for the midazolam sample preparation were obtained from Biosolve (Valkenswaard, the Netherlands). HPLC grade H_2O, MeOH, ethanol (EtOH), and HCOOH used for the plasma sample preparation procedure were obtained from Sigma-Aldrich (St. Louis, USA).

Sample preparation

Reference standards of phenylalanine and caffeine were dissolved in LC-MS grade H_2O (~1 µM) and directly used for LC-IRIS analysis. Midazolam was incubated at 10 µM for 120 minutes in human hepatocytes. The final hepatocyte density was 10^6 cells/ml. A 40 µl incubation volume was quenched with two volumes of ACN/HCOOH 90:10 [v/v] and the sample was centrifuged for 10 minutes at 4000 rpm. The supernatant was used for LC-IRIS analysis. A plasma sample from a patient with the inborn error of metabolism pyridoxine-dependent epilepsy (PDE-ALDHA7A1), stored at -80 °C, was thawed at 4 °C. 100 µl of sample was combined with 400 µl of ice-cold MeOH/EtOH 50:50 [v/v], mixed with a vortex mixer and incubated for 20 min at 4 °C. The mixture was centrifuged for 15 min at 4 °C and 18600 g. The supernatant (350 µl) was dried in a centrifugal vacuum evaporator (Eppendorf) and reconstituted in 100 µl of H_2O/MeOH 90:10 [v/v] with 0.1% HCOOH. The sample was mixed for 15 s with a vortex mixer and centrifuged for 15 min at 18600 g (room temperature). The supernatant was used for LC-IRIS analysis.

Liquid chromatography

LC separations were performed with a Bruker Elute UHPLC system consisting of a binary pump, cooled autosampler and column oven. The outlet of the column was connected to the heartcutting LC-IRIS interface (see next section). Separations were performed with a Waters Acquity HSS T3 C18 column (100 × 2.1 mm i.d., 1.8 µm particles, 100 Å pore size) held at 40 °C and mobile phases consisting of 10 mM CH_3COOH in H_2O (mobile phase A) and 10 mM CH_3COOH in MeOH (mobile phase B). After an initial time of 1 min at 99% A, a gradient was run to 100% B in 15 min, followed by a hold at 100% B for 2 minutes. An equilibration time of 2 minutes was used between injections. The flow rate was 0.35 ml/min and an injection volume of 2 µl was used for all samples.

Heartcutting liquid chromatography – infrared ion spectroscopy interface

A schematic representation of the heartcutting LC-IRIS interface is shown in Figure 1. The interface consists of a 6-position 7-port selector valve (PD7970 TitanHP™ pod, Idex) and a 2-position 10-port switching valve (PD9960 TitanHP™ pod, Idex). Both valves and drivers (MHP0267-500-1 TitanHP™ actuator, Idex) were installed in a home-built switching box (see Figure 2a). The switching box is under hardware control of the PC used to operate the MS via a USB connection. Synchronization of the experiment is done via an in-house developed LabView program that sends down commands to the switching box and to the ion trap via the low-level Atlas development interface. The LabView program contains a timed command queue that controls all events, which starts when the ion trap control program (trapControl, Bruker) switches to acquisition mode (i.e. at the start of an LC-MS experiment). The program requires a timetable of events (i.e. switching of a specific valve) that take place during an experimental run as user input.

As shown in Figure 1, the column outlet is connected to position 7 of the selector valve (V1), allowing the eluent to go to the ESI source of the ion trap (panel a), to the second valve (V2, panel b and c) or to waste (panel d and e). At the start of a heartcutting LC-IRIS experiment, V1 is in the first position (7-1, panel a), allowing regular LC-MS analysis. As soon as a fraction containing an ion of interest elutes from the column, V1 is switched (7-5, panel b) and the eluent is sent to V2, which is equipped with two sample loops. The fraction of eluent is stored in one of the sample loops and, subsequently, V1 is switched back to continue LC-MS analysis. When a second peak of interest elutes from the column, both V1 and V2 are switched (panel c) and the second sample loop is filled. After the peak, V1 can be switched back to monitor the final part of the LC run. This step may be skipped to save time. For IRIS analysis, V1 is switched (7-2, panel d) to send the eluent to waste. During this time, the column can be equilibrated to prepare for the next injection. The syringe, installed on the 10^{th} position of V2 is turned on to deliver a constant flow rate that can be significantly lower than the flow rate used for the LC-separation. Depending on the position of V2 the fraction stored in either the first loop (panel d) or the second loop (panel e) is slowly infused to the ESI source of the ion trap,

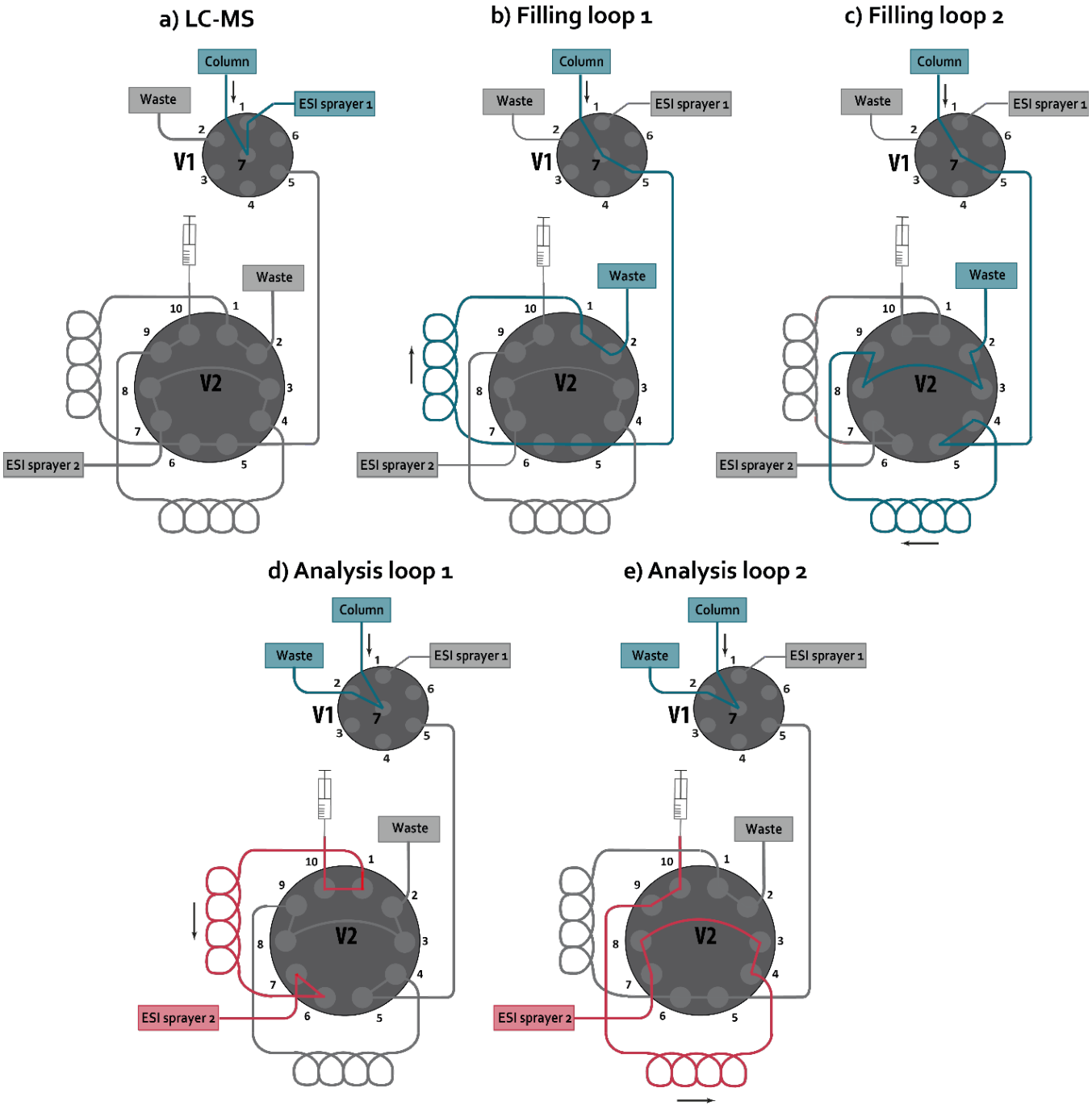

Figure 1. Schematic representation of the heartcutting LC-IRIS interface consisting of a 6-position 7-port selector valve (V1) and a 2-position 10-port switching valve (V2). The valves can be positioned to (a) perform regular LC-MS analysis, (b) fill the first sample loop with eluent, (c) fill the second sample loop with eluent, (d) infuse the contents of the first sample loop to the MS instrument or (e) infuse the contents of the second sample loop to the MS

generating an ion signal for IRIS analysis. Note that the setup was designed to fill and empty the loops in opposite direction ("backflush" mode) to minimize band spreading. After IRIS analysis, V1 and V2 can be switched to allow the mobile phase flow to go through each of the loops (panel b and d) for a few minutes to clean the sample loops for the next analysis.

The ESI source installed on the ion trap should receive flow from two different parts of the setup shown in Figure 1 (port 1 of V1 and port 7 of V2). To enable this, we modified the Apollo ESI source standardly installed on the amaZon speed ion trap MS. When not using the heartcutting setup, the source receives flow via an ESI sprayer installed at the top of the housing and two windows are installed on the left and right sides. In this setup, we removed those windows and installed ESI sprayers on both sides of the source and one of the windows was placed on the top of the source (see Figure 2b). This allows the ESI sprayers to be separately optimized to receive flow from two different sources at different flow rates; the needle extension of one ESI sprayer (connected to port 1 of V1) was optimized for the high flows received directly from the LC system during LC-MS analysis and the other sprayer was optimized for the lower flows received from port 7 of V2 during IRIS analysis. Additionally, the standard nebulizer gas (N_2) delivered by the amaZon speed instrument was used to assist ESI at the low-flow sprayer and

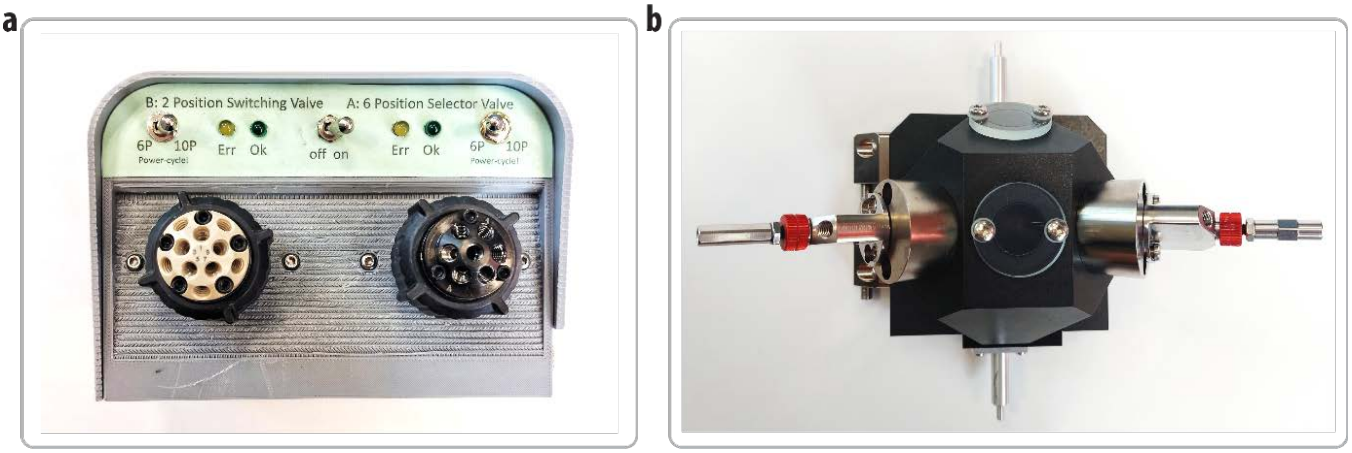

Figure 2. Photos of (a) the homebuilt valve switching box holding V1 (right) and V2 (left) and (b) modified Apollo ESI source holding two ESI sprayers.

an additional external gas controller (E-5752-AAA, Bronkhorst HI-TEC) was installed to deliver a flow of 400 L/hr to the higher-flow sprayer. Both N_2-flows arrive in the same spray chamber and therefore they influence the ESI process at both sprayers. We determined that the best ion signals are obtained when the external gas controller (delivering N_2 to the high-flow sprayer) is turned off during the IRIS experiments (panel d and e in Figure 1).

Collision induced dissociation and infrared ion spectroscopy experiments

All experiments were performed using a 3D ion trap mass spectrometer (Bruker, amaZon speed ETD) that was modified for IRIS experiments using the FELIX free electron laser (see Ref. [39]). Although the heartcutting LC-IRIS set-up described here is designed to record IR spectra via photodissociation MS/MS, we also used collision-induced dissociation (CID) for a preliminary evaluation of the set-up (avoiding use of costly FELIX beam time) or to monitor the signal before the start of an LC-IRIS experiment. Here, 28-40 ms of CID was used. The CID amplitude was adapted to each ion. The CID fragmentation yield was calculated by relating the fragment and precursor ion intensities (fragmentation yield = $I_{fragment}$ / $I_{fragment}$ + $I_{precursor}$).

For IRIS experiments, FELIX was set to produce 10 Hz macropulses of duration 5-10 µs and energy 10-80 mJ (varying with wavelength) in the 650-1900 cm^{-1} region. The bandwidth was ~0.4% of the central frequency. Ions of interest were mass-isolated and irradiated using a single macropulse. When the laser is on resonance with a vibrational transition of the ions, resonant absorption occurs and leads to an increase of ion internal energy followed by unimolecular dissociation. This was detected by recording an MS spectrum after irradiation. To acquire an IR spectrum, FELIX was stepped through the wavelength range (in 5 cm^{-1} steps) while recording an MS/MS spectrum at each wavelength point (taking 6 averages at each point). Analogous to the CID experiments, IR spectra were generated by plotting the IR-induced fragmentation yield as function of laser frequency. Here, the IR wavelength was calibrated using a grating spectrometer. Usually, when comparing IRIS spectra to linear absorption spectra (such as obtained from quantum-chemical calculations), the intensity is calculated via: IRIS intensity = ln(ΣI(precursor + fragment ions)/I(precursor ion)) and IRIS intensities are corrected for frequency-dependent laser pulse energy variations.[40] IR spectra calculated in this manner can be found in the supporting information (Figure S1-S3).

RESULTS AND DISCUSSION

Evaluation of the heartcutting LC-IRIS set-up

We prepared a mixture (~1 µM in H_2O) of the compounds tryptophan, phenylalanine and caffeine to evaluate the performance of the heartcutting LC-IRIS set-up. All compounds were primarily detected as protonated structures ($[M+H]^+$) in positive electrospray ionization mode (+ESI). The heartcutting LC-IRIS setup enables not only the recording of IR spectra, but also the recording of LC-MS chromatograms (with gaps corresponding to the heartcuts) in the same experiment. These can be used for quality-control purposes (i.e. to detect bad injections or retention time drifts). We used the signal of protonated phenylalanine (*m/z* 166) to demonstrate this. The peaks containing protonated tryptophan (*m/z* 205) and protonated caffeine (*m/z* 195) were stored in the sample loops for MS/MS analysis. In MS/MS experiments (both CID and IRMPD), protonated tryptophan produces a main fragment at *m/z* 188, whereas caffeine mainly fragments towards *m/z* 138. Reference IRIS spectra of both compounds recorded using direct-infusion ESI are shown in Figure 3e. The mixture was separated using a reversed phase LC-MS method (see method section) and extracted ion chromatograms (EICs) of *m/z* 166 (phenylalanine), *m/z* 205 (tryptophan) and *m/z* 195 (caffeine) are shown in Figure 3a with retention times of ~3.9 minutes, ~5.1 minutes and ~6.9 minutes, respectively (the peak widths are ~0.13 minutes). Setting up an LC-IRIS experiment for the analysis of phenylalanine and caffeine includes selecting an appropriate sample loop and determining the switching times of V1 and V2. When selecting a sample loop, it is important to note that the linear velocity of solvent flowing through a small tube is approximately twice as high at the centre of the tube as the average linear velocity (laminar flow[36, 41]). Selecting a sample loop that exactly fits the LC peak (loop size = LC flow rate x peak width) will therefore lead to sample losses. On the other hand, we found that if the loop is much larger than the stored fraction,

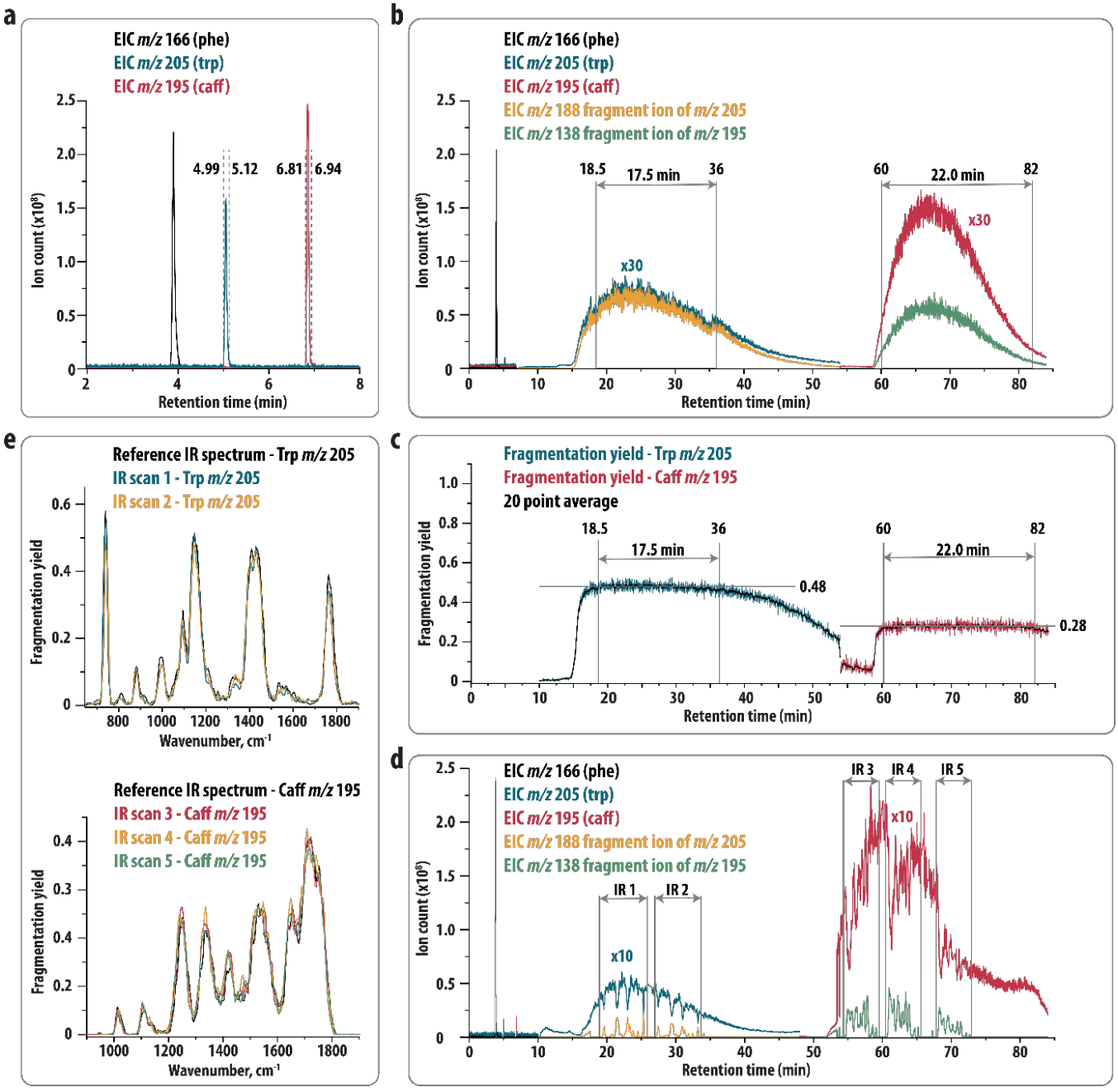

Figure 3. (a) EICs resulting from the LC-MS analysis of a mixture of Phe (*m/z* 166), Trp (*m/z* 205) and Caff (*m/z* 195). The dashed vertical lines indicate the switching times of the valves leading to the storage of the Trp fraction in sample loop 1 and the Caff fraction in sample loop 2. (b) EICs resulting from the analysis of the mixture using the heartcutting LC-IRIS set-up and CID with a constant CID amplitude. EICs during the loop analysis (>6.94 minutes) are scaled by 30 for better visualisation. (c) Amount of fragmentation of Trp and Caff observed during the analysis shown in (b). The region in which the fragmentation yield is stable is indicated. (d) EICs resulting from the analysis of a mixture of Phe (*m/z* 166), Trp (*m/z* 205) and Caff (*m/z* 195) using the heartcutting LC-IRIS set-up and IRIS. The start and end of each IR scan is indicated. EICs during the analysis of the loops (>10 minutes) are scaled by 10 for better visualisation. (e) IR spectra resulting from the IRIS analysis shown in (d) compared to reference IR spectra obtained in a direct infusion experiment.

i.e. if parts of the loop are filled with mobile phase eluent from the previous run, interference with isobaric background ions can occur. Therefore, we generally select a sample loop that is 30 percent larger than the theoretical size of the analyte fraction (following best practices of the 2D-LC community [36]). In the case described here, the LC flow rate was 350 µl/min and the peak width ~0.13 minutes, which yields a fraction size of 45.5 µl. Therefore, we selected commercially available samples loops of 60 µl (≈1.3 x 45.5 µl). Absolute switching times of the valves were determined to store the central part of the peak in the sample loop, as indicated by the dashed lines in Figure 3a.We infused the stored fractions into the MS with a syringe pump flow rate of 150 µl/h (=2.5 µl/min), which generally gives a stable signal. Note that this flow rate is 140 times lower than the LC flow rate, so that we could theoretically have 18 minutes of ion signal (0.13 x 140) from

each fraction for IRIS experiments. To determine the exact time window in which the signal is stable enough to allow IRIS experiments, we first performed a simple CID fragmentation experiment. During the elution of each analyte fraction, we set the ion trap to constantly perform mass isolation (*m/z* 205 for the tryptophan fraction and *m/z* 195 for the caffeine fraction) and CID fragmentation at a constant CID amplitude (0.3 V for tryptophan, 0.46 V for caffeine). Figure 3b shows the EICs corresponding to protonated phenylalanine and the precursor and main fragment ion of protonated tryptophan and caffeine. Here, t=0 corresponds to the start of the LC run. The first 6.94 minutes of the figure correspond to the LC-MS analysis showing that phenylalanine (*m/z* 166) elutes normally as a sharp peak and the correct retention time, while at the elution times of tryptophan and caffeine (corresponding with the valve switching times) no peak is observed, because fractions are diverted into the sample loops. After the second sample loop is filled (6.94 minutes), the valves are switched to infuse the contents of the first sample loop into the ion trap, which is set to mass-isolate and fragment tryptophan. Over a range of ~40 minutes, signals corresponding to the precursor ion (*m/z* 205) and main fragment ion (*m/z* 188) of tryptophan are observed.

To determine the time window for IRIS experiments, we calculated the fragmentation yield, which should be constant at a constant CID amplitude. This is shown in Figure 3c, indicating a stable yield between ~18.5 minutes and ~36 minutes, so that we have ~17.5 minutes to reliably perform IRIS experiments. At 54 minutes, V2 was switched to infuse the contents of the second sample loop, while mass-isolating and fragmenting *m/z* 195 (protonated caffeine). Here, a signal for the precursor and main fragment ion was observed from ~59-85 minutes (Figure 3b) and a stable yield was observed from ~60-82 minutes (22 minutes, Figure 3c). This is longer than for tryptophan, which may be related to the higher signal intensity for caffeine as was also observed in the LC-MS analysis (Figure 3a). This is also longer than the theoretical 18 minutes (see above), indicating that some peak broadening takes place during the infusion of the loop contents. Note that the loss of sensitivity is not simply equal to the decrease in flow rate, as the ion trap partially corrects for the lower flow by increasing the ion accumulation time (from <0.01 ms during the LC-MS elution to 3-20 ms during the loop analysis). The ion counts are corrected by the ion accumulation time, giving the signals during the loop analysis a much lower apparent signal. Therefore, we magnified all signals during the loop analysis (see Figure 3) for better visualisation. The actual total ion counts recorded by the ion trap were found to be only 2-5 times lower during the loop analysis, where we note that no mass-isolation took place during the LC-MS run and the total ion count was distributed over many *m/z*-peaks. Therefore, for analytes with a moderate concentration, the loop-analysis can have sensitivities comparable to regular LC-MS, as mass-isolation allows a >100 times higher ion accumulation time.

With the valve switching times determined, the experiment was repeated using IRIS instead of CID. The EICs are shown in Figure 3d. Note here that in this case the analysis of the loops was started somewhat later (at 10 minutes) than in panel b, leading to a shift of all signals by a few minutes. Here, fragmentation was induced by the IR laser (see method section), which was stepped through the IR fingerprint range (1900-650 cm^{-1} for tryptophan and 1900-900 cm^{-1} for caffeine, in 5 cm^{-1} steps); each point in the loop analysis indicates a different wavelength point of the laser. We were able to perform two IR scans for protonated tryptophan and three for protonated caffeine in a single LC run. The start and the end of each IR scan is indicated in Figure 3d. In this case, fragment ions are not constantly observed, but rather appear in peaks, indicating points where the IR laser is on resonance with a vibrational transition in the precursor ion. Figure 3e compares the IR spectra obtained in this manner to reference IR spectra obtained in a direct-infusion experiment, showing that the spectra match closely.

Proof-of-concept I. Identification of phase I and phase II drug metabolites

LC-MS is commonly applied to the characterisation of downstream metabolites of drug compounds during drug discovery and development.[42-44] However, using MS for the identification of drug metabolite structures comes with challenges, i.e. the type of metabolic transformation that takes place can often be inferred from the mass difference between the drug and the metabolite, but the exact site of a biotransformation is often difficult to determine. We recently showed the application of IRIS in drug metabolite profiling by identifying metabolites of the drug midazolam (MDZ).[45] Midazolam undergoes a hydroxylation reaction, resulting in 1'-hydroxymidazolam (1'-OH-MDZ, *m/z* 342), which undergoes a second metabolic reaction to form a glucuronide, 1'-hydroxymidazolam-O-glucuronide (1'-OH-MDZ-O-gluc, *m/z* 518, see Figure 4a). Identification of the metabolites of MDZ involved recording IR spectra of the two ions, but also of the glucuronide-loss CID MS/MS fragment (the aglycone) of 1'-OH-MDZ-O-gluc. This fragment is expected to be identical to 1'-OH-MDZ (see Fig 4a) and its IR spectrum was therefore compared with the 1'-OH-MDZ spectrum to establish a link between the two metabolites, revealing the position of the OH-group in 1'-OH-MDZ-O-gluc. Moreover, the IR absorption bands of these metabolites have a large variation in absorption cross-section, so that multiple IR scans were recorded at different laser power settings to detect all IR features and to prevent excessive ion depletion at strong vibrational transitions. It was therefore necessary to perform multiple (LC-)experiments to record all required IR spectra.

Here we repeated the experiments on MDZ to demonstrate that all required IR spectra, involving different settings of the laser beam attenuation, can be measured from a single LC injection using the heartcutting LC-IRIS set-up. Figure 4b contains the results of an LC-MS analysis, showing the elution of protonated MDZ (*m/z* 326), 1'-OH-MDZ-O-gluc (*m/z* 518) and 1'-OH-MDZ (*m/z* 342). The valves were set to switch at appropriate times to store the *m/z* 518 fraction in the first loop and the *m/z* 342 fraction in second loop (indicated by the dashed grey lines). Figure 4c shows several EICs recorded during the heartcutting LC-IRIS experiment, where the start and end of each of the six IR scans are indicated in the figure. At several time points during the analysis, fragmentation using CID was performed to check the signal stability (also indicated in Figure 4c). During the first part of the analysis of the first loop, *m/z* 518 is mass-isolated and irradiated, leading to dissociation into multiple fragments. For clarity, only the

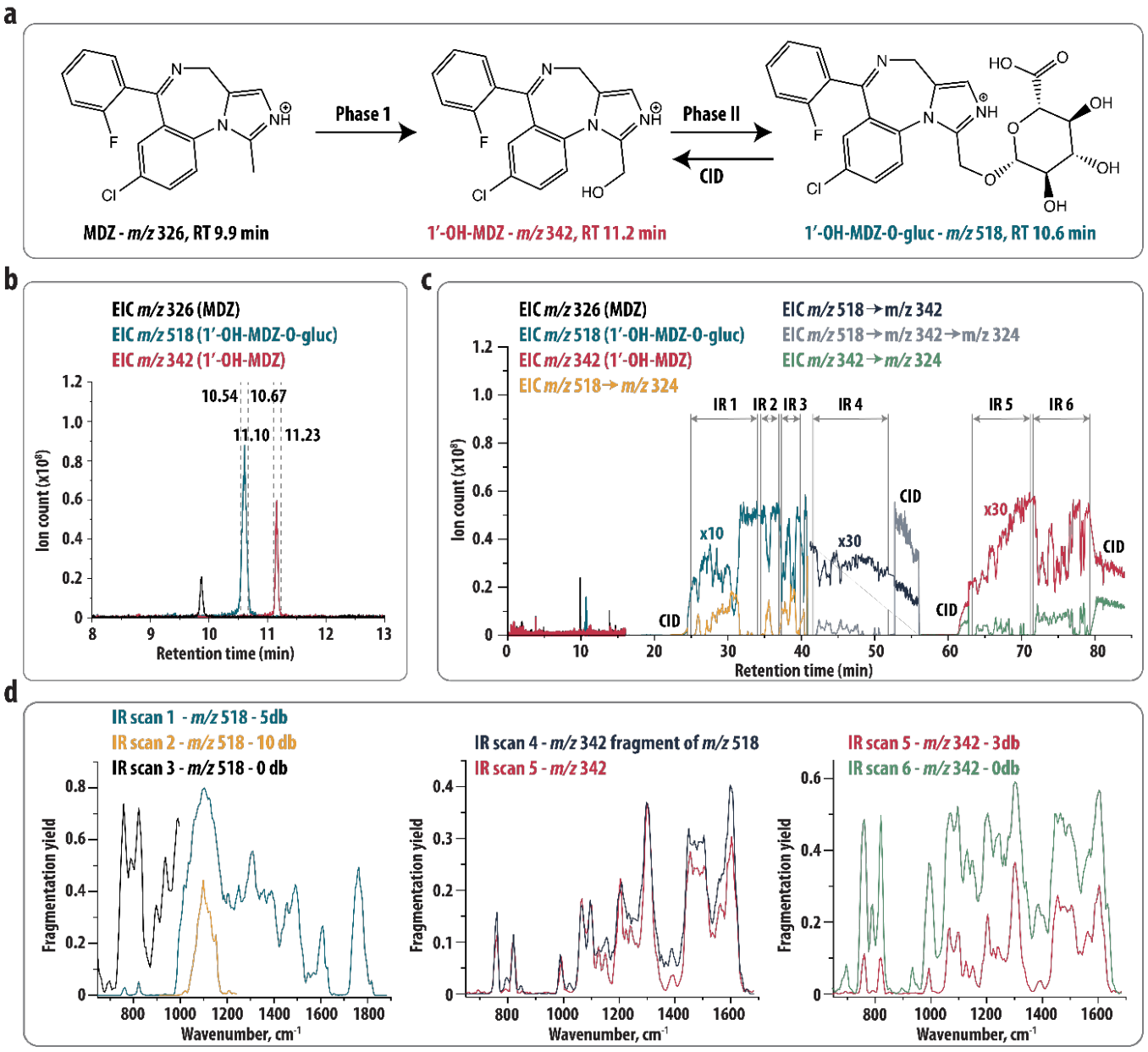

Figure 4. (a) Metabolism of MDZ. Phase I metabolism involves a hydroxylation reaction (+16 MW) leading to 1'-OH-MDZ, which is further metabolized in a glucuronide resulting in 1'-OH-MDZ-O-gluc. Protonated structures are shown. (b) EICs resulting from the LC-MS analysis of a MDZ incubation sample. The elution of protonated MDZ, 1'-OH-MDZ and 1'-OH-MDZ-O-gluc is observed. Dashed vertical lines indicate the switching times of the valves leading to the storage of the 1'-OH-MDZ-O-gluc and 1'-OH-MDZ fraction in sample loop 1 and 2, respectively. (d) EICs resulting from the analysis of the MDZ incubation sample using the heartcutting LC-IRIS set-up. The start and end of each IR scan is indicated. EICs during the analysis of the loops (>16 minutes) are scaled by a factor of 10 and 30 for better visualisation. Time windows in which CID is performed are indicated. (d) IR spectra resulting from the IRIS analysis shown in (c). IR laser intensities are labeled with the amount of laser attenuation in dB where 0, 3, 5, 10 dB correspond to 100, 50, 31.6 and 10% of the maximum laser intensity.

EIC of the most intense fragment ion (*m/z* 324) is presented. Three R scans were performed at different IR laser intensities. The IR spectra resulting from this IRIS analysis (presented as the yield of all fragment ions) are shown in Figure 4d (left panel). Subsequently, *m/z* 518 was mass-isolated and fragmented by CID to the *m/z* 342 ion, which was mass-isolated and irradiated by FELIX; Figure 4c shows the EIC of the main IRMPD fragment ion at *m/z* 324. During the infusion of the second loop, *m/z* 342 was mass-isolated and its IRIS spectrum is compared to the IR spectrum of the *m/z* 342 fragment ion from the *m/z* 518 precursor in the middle panel of Figure 4d, indicating that these ions indeed possess the same IR spectrum and hence correspond to the same structure. The IR analysis of the *m/z* 342 ion was repeated using a higher laser power to pick up the low-intensity bands, as shown in the right panel of Figure 4d.

Proof-of-concept II. Identifying diastereomeric biomarkers for pyridoxine dependent epilepsy

Untargeted metabolomics strategies based on LC-MS are routinely employed in the clinical laboratory to search for new biomarkers for a variety of medical conditions.[46-49] An

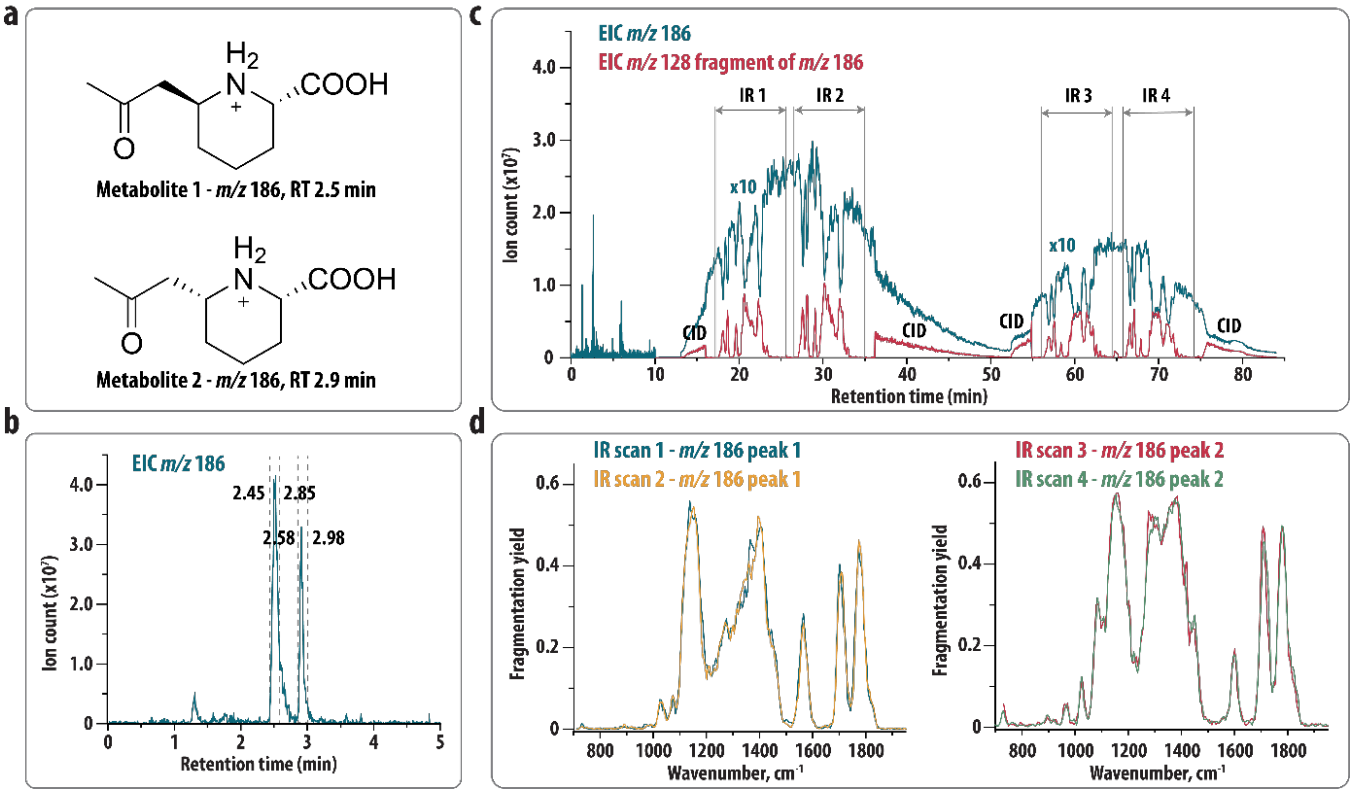

Figure 5. (a) Diastereomeric metabolite biomarkers (*m/z* 186) for PDE-ALDH7A1. (b) EICs resulting from the LC-MS analysis of a PDE plasma sample showing the elution of the two biomarkers. The dashed vertical lines indicate the switching times of the valves leading to the storage of metabolites 1 and 2 in sample loop 1 and 2, respectively. (c) EICs resulting from the analysis of the plasma sample using the heartcutting LC-IRIS set-up. The start and end of each IR scan is indicated. EICs during the analysis of the loops (>10 minutes) are scaled by a factor of 10 for better visualisation. Time windows where CID is performed to verify the ion signal are indicated. (d) IR spectra resulting from the IRIS analysis in (c).

example is the field of inborn errors of metabolism, where metabolite identification is crucial to establish a pathophysiological understanding of these diseases and to discover biomarkers for diagnostics.[48, 49] However, structural elucidation of the metabolites detected by LC-MS remains a major bottleneck and the application of LC-IRIS has therefore recently been explored in this context.[29, 50] Pyridoxine dependent epilepsy (PDE-ALDH7A1) is an inborn error of metabolism leading to severe epilepsy in newborns.[51, 52] It is known to be caused by the deficiency of the enzyme antiquitin, causing the accumulation of several metabolites in the lysine pathway.[53] Recently, IRIS was used to identify two novel metabolites associated with PDE-ALDH7A1 (structures shown in Figure 5a).[29, 50] These biomarkers are diastereomers and have very similar retention in a reversed-phase LC separation (see Figure 5b). Obtaining isolated fractions that contain only one of the diastereomers is therefore challenging using a fraction collection set-up and likely impossible using stop-flow chromatography.

Using the heartcutting LC-IRIS set-up, the first and second metabolite peak (both *m/z* 186) were stored in the first and second sample loop, respectively. Switching times of the two valves are indicated by the dashed grey lines in Figure 5b and Figure 5c shows several EICs recorded during the heartcutting LC-IRIS experiment, demonstrating that we were able to obtain two IR spectra for each of the metabolites. Both metabolites primarily dissociate towards an ion with *m/z* 128 and the resulting IR spectra are shown in Figure 5d. These results confirm that there is no carryover between the two IR spectra; for instance, the peak at 1550 cm^{-1} in the spectrum of the first eluting feature is completely absent in the IR spectrum of the second eluting feature. In a previous study,[50] the concentration of the two metabolites in PDE-ALDH7A1 patient plasma was determined to be ~3 µM.

CONCLUSIONS

In recent years, IRIS is increasingly recognized as a molecular identification tool in MS-based analytical workflows and has seen application in multiple (bio)chemical research areas. However, many analytical workflows combine MS with LC-separation, whereas the direct coupling of LC and IRIS is difficult because of the mismatching timescales of the two technologies: an IRIS run takes much longer than the width of a typical LC peak. Here we present a heartcutting LC-IRIS set-up as a novel approach to analytical LC-IRIS. Using this set-up, fractions of analytes eluting from an LC column can be stored in a sample loop and infused into the MS instrument at a reduced flow rate, elongating the analyte signal to ~20 minutes. This enables the acquisition of several IR spectra for each analyte, allowing for spectral averaging for improved data quality or for the acquisition of spectra under different experimental conditions (e.g. various laser pulse energies, fragment ion IR spectra, etc.). This leads to lower sample consumption as two *m/z*-features can be fully characterized from a single (~µl) injection of sample. The set-up is largely automated using a LabVIEW program and does not require user input up to the start of the IRIS scan. Here, we have

demonstrated the approach by showing examples from the field of drug metabolism and the field of inborn errors of metabolism, but also envision applications in other fields where the identification of molecular structures detected by LC-MS is required. In both applications, we demonstrated identification of multiple analytes from a single LC injection, including a partial bottom-up structural elucidation via the recording of an IR spectrum of a fragment ion. Our set-up for IRIS employs a free-electron laser, but the heartcutting LC-IRIS method is also directly suitable for experiments with other IR lasers, such as table-top optical parametric oscillators (OPOs)[54] or other types of MS-integrated spectroscopy experiments[55, 56]. Using additional and/or different types of switching valves, the setup can as well be expanded with additional sample loops to allow the analysis of more than two analytes per LC injection.

ASSOCIATED CONTENT

Supporting information

IRIS spectra. This material is available free of charge via the Internet at http://pubs.acs.org.

AUTHOR INFORMATION

Corresponding Author

***jonathan.martens@ru.nl (J.Ma)**

Notes

The authors declare no competing financial interest. All data are included in the manuscript and the Supporting Information. Raw research data are available upon request from the corresponding authors.

ACKNOWLEDGEMENTS

The authors gratefully acknowledge the excellent technical assistance from the FELIX group. We thank the Nederlandse Organisatie voor Wetenschappelijk Onderzoek (NWO) for the support of the FELIX Laboratory. Financial support for this project was provided by NWO Chemical Sciences under projects NWO-TTW nr. 15769 and TKI-LIFT nr. 731.017.419.

References

1. Cui, L.; Lu, H.; Lee, Y. H., Challenges and emergent solutions for LC-MS/MS based untargeted metabolomics in diseases. *Mass Spectrometry Reviews* **2018,** *37*, 772-792.
2. Dunn, W. B.; Erban, A.; Weber, R. J. M.; Creek, D. J.; Brown, M.; Breitling, R.; Hankemeier, T.; Goodacre, R.; Neumann, S.; Kopka, J.; Viant, M. R., Mass appeal: metabolite identification in mass spectrometry-focused untargeted metabolomics. *Metabolomics* **2013,** *9*, 44-66.
3. Heiles, S., Advanced tandem mass spectrometry in metabolomics and lipidomics—methods and applications. *Analytical and Bioanalytical Chemistry* **2021,** *413*, 5927-5948.
4. De Vijlder, T.; Valkenborg, D.; Lemière, F.; Romijn, E. P.; Laukens, K.; Cuyckens, F., A tutorial in small molecule identification via electrospray ionization-mass spectrometry: The practical art of structural elucidation. *Mass Spectrometry Reviews* **2018,** *37*, 607-629.
5. Kind, T.; Fiehn, O., Advances in structure elucidation of small molecules using mass spectrometry. *Bioanalytical Reviews* **2010,** *2*, 23-60.
6. Hufsky, F.; Böcker, S., Mining molecular structure databases: Identification of small molecules based on fragmentation mass spectrometry data. *Mass Spectrometry Reviews* **2017,** *36*, 624-633.
7. Lapthorn, C.; Pullen, F.; Chowdhry, B. Z., Ion mobility spectrometry-mass spectrometry (IMS-MS) of small molecules: Separating and assigning structures to ions. *Mass Spectrometry Reviews* **2013,** *32*, 43-71.
8. Gika, H. G.; Theodoridis, G. A.; Plumb, R. S.; Wilson, I. D., Current practice of liquid chromatography–mass spectrometry in metabolomics and metabonomics. *Journal of Pharmaceutical and Biomedical Analysis* **2014,** *87*, 12-25.
9. Beale, D. J.; Pinu, F. R.; Kouremenos, K. A.; Poojary, M. M.; Narayana, V. K.; Boughton, B. A.; Kanojia, K.; Dayalan, S.; Jones, O. A. H.; Dias, D. A., Review of recent developments in GC–MS approaches to metabolomics-based research. *Metabolomics* **2018,** *14*, 152.
10. Lemaire, J.; Boissel, P.; Heninger, M.; Mauclaire, G.; Bellec, G.; Mestdagh, H.; Simon, A.; Caer, S. L.; Ortega, J. M.; Glotin, F.; Maitre, P., Gas Phase Infrared Spectroscopy of Selectively Prepared Ions. *Physical Review Letters* **2002,** *89*, 273002.
11. Oomens, J.; Sartakov, B. G.; Meijer, G.; von Helden, G., Gas-phase infrared multiple photon dissociation spectroscopy of mass-selected molecular ions. *International Journal of Mass Spectrometry* **2006,** *254*, 1-19.
12. Fridgen, T. D., Infrared consequence spectroscopy of gaseous protonated and metal ion cationized complexes. *Mass Spectrometry Reviews* **2009,** *28*, 586-607.
13. Martens, J.; Berden, G.; Oomens, J., Structures of Fluoranthene Reagent Anions Used in Electron Transfer Dissociation and Proton Transfer Reaction Tandem Mass Spectrometry. *Analytical Chemistry* **2016,** *88*, 6126-6129.
14. Polfer, N. C., Infrared multiple photon dissociation spectroscopy of trapped ions. *Chemical Society Reviews* **2011,** *40*, 2211-2221.
15. Polfer, N. C.; Oomens, J., Vibrational spectroscopy of bare and solvated ionic complexes of biological relevance. *Mass Spectrometry Reviews* **2009,** *28*, 468-494.
16. Carlo, M. J.; Patrick, A. L., Infrared multiple photon dissociation (IRMPD) spectroscopy and its potential for the clinical laboratory. *Journal of Mass Spectrometry and Advances in the Clinical Lab* **2022,** *23*, 14-25.
17. Maitre, P.; Scuderi, D.; Corinti, D.; Chiavarino, B.; Crestoni, M. E.; Fornarini, S., Applications of Infrared Multiple Photon Dissociation (IRMPD) to the Detection of Posttranslational Modifications. *Chemical Reviews* **2020,** *120*, 3261-3295.
18. Kranenburg, R. F.; van Geenen, F. A. M. G.; Berden, G.; Oomens, J.; Martens, J.; van Asten, A. C., Mass-Spectrometry-Based Identification of Synthetic Drug Isomers Using Infrared Ion Spectroscopy. *Analytical Chemistry* **2020,** *92*, 7282-7288.
19. Bell, M. R.; Tesler, L. F.; Polfer, N. C., Cryogenic infrared ion spectroscopy for the structural elucidation of drug molecules: MDMA and its metabolites. *International Journal of Mass Spectrometry* **2019,** *443*, 101-108.
20. Tyler Davidson, J.; Piacentino, E. L.; Sasiene, Z. J.; Abiedalla, Y.; DeRuiter, J.; Clark, C. R.; Berden, G.; Oomens, J.; Ryzhov, V.; Jackson, G. P., Identification of novel fragmentation pathways and fragment ion structures in the tandem mass spectra of protonated synthetic cathinones. *Forensic Chemistry* **2020,** *19*, 100245.
21. van Geenen, F. A. M. G.; Kranenburg, R. F.; van Asten, A. C.; Martens, J.; Oomens, J.; Berden, G., Isomer-Specific Two-Color Double-Resonance IR2MS3 Ion Spectroscopy Using a Single Laser: Application in the Identification of Novel

Psychoactive Substances. *Analytical Chemistry* **2021,** *93*, 2687-2693.
22. Vo, L.; Legaard, E.; Thrasher, C.; Jaffe, A.; Berden, G.; Martens, J.; Oomens, J.; O'Brien, R. E., UV/Vis and IRMPD Spectroscopic Analysis of the Absorption Properties of Methylglyoxal Brown Carbon. *ACS Earth and Space Chemistry* **2021,** *5*, 910-919.
23. Walhout, E. Q.; Dorn, S. E.; Martens, J.; Berden, G.; Oomens, J.; Cheong, P. H. Y.; Kroll, J. H.; O'Brien, R. E., Infrared Ion Spectroscopy of Environmental Organic Mixtures: Probing the Composition of α-Pinene Secondary Organic Aerosol. *Environmental Science & Technology* **2019,** *53*, 7604-7612.
24. Vink, M. J. A.; van Geenen, F. A. M. G.; Berden, G.; O'Riordan, T. J. C.; Howe, P. W. A.; Oomens, J.; Perry, S. J.; Martens, J., Structural Elucidation of Agrochemicals and Related Derivatives Using Infrared Ion Spectroscopy. *Environmental Science & Technology* **2022**.
25. Martens, J.; van Outersterp, R. E.; Vreeken, R. J.; Cuyckens, F.; Coene, K. L. M.; Engelke, U. F.; Kluijtmans, L. A. J.; Wevers, R. A.; Buydens, L. M. C.; Redlich, B.; Berden, G.; Oomens, J., Infrared ion spectroscopy: New opportunities for small-molecule identification in mass spectrometry - A tutorial perspective. *Analytica Chimica Acta* **2020,** *1093*, 1-15.
26. van Outersterp, R. E.; Martens, J.; Berden, G.; Koppen, V.; Cuyckens, F.; Oomens, J., Mass spectrometry-based identification of ortho-, meta- and para-isomers using infrared ion spectroscopy. *Analyst* **2020,** *145*, 6162-6170.
27. Martens, J.; Koppen, V.; Berden, G.; Cuyckens, F.; Oomens, J., Combined Liquid Chromatography-Infrared Ion Spectroscopy for Identification of Regioisomeric Drug Metabolites. *Anal. Chem.* **2017,** *89*, 4359-4362.
28. van Outersterp, R. E.; Moons, S. J.; Engelke, U. F. H.; Bentlage, H.; Peters, T. M. A.; van Rooij, A.; Huigen, M. C. D. G.; de Boer, S.; van der Heeft, E.; Kluijtmans, L. A. J.; van Karnebeek, C. D. M.; Wevers, R. A.; Berden, G.; Oomens, J.; Boltje, T. J.; Coene, K. L. M.; Martens, J., Amadori rearrangement products as potential biomarkers for inborn errors of amino-acid metabolism. *Communications Biology* **2021,** *4*, 367.
29. van Outersterp, R. E.; Engelke, U. F. H.; Merx, J.; Berden, G.; Paul, M.; Thomulka, T.; Berkessel, A.; Huigen, M. C. D. G.; Kluijtmans, L. A. J.; Mecinović, J.; Rutjes, F. P. J. T.; van Karnebeek, C. D. M.; Wevers, R. A.; Boltje, T. J.; Coene, K. L. M.; Martens, J.; Oomens, J., Metabolite Identification Using Infrared Ion Spectroscopy─Novel Biomarkers for Pyridoxine-Dependent Epilepsy. *Analytical Chemistry* **2021,** *93*, 15340-15348.
30. Lee, M. S.; Kerns, E. H., LC/MS applications in drug development. *Mass Spectrometry Reviews* **1999,** *18*, 187-279.
31. Seger, C.; Salzmann, L., After another decade: LC–MS/MS became routine in clinical diagnostics. *Clinical Biochemistry* **2020,** *82*, 2-11.
32. Dunn, W. B.; Broadhurst, D.; Begley, P.; Zelena, E.; Francis-McIntyre, S.; Anderson, N.; Brown, M.; Knowles, J. D.; Halsall, A.; Haselden, J. N.; Nicholls, A. W.; Wilson, I. D.; Kell, D. B.; Goodacre, R.; The Human Serum Metabolome, C., Procedures for large-scale metabolic profiling of serum and plasma using gas chromatography and liquid chromatography coupled to mass spectrometry. *Nature Protocols* **2011,** *6*, 1060-1083.
33. van Outersterp, R. E.; Houthuijs, K. J.; Berden, G.; Engelke, U. F.; Kluijtmans, L. A. J.; Wevers, R. A.; Coene, K. L. M.; Oomens, J.; Martens, J., Reference-standard free metabolite identification using infrared ion spectroscopy. *International Journal of Mass Spectrometry* **2019,** *443*, 77-85.
34. Schindler, B.; Laloy-Borgna, G.; Barnes, L.; Allouche, A.-R.; Bouju, E.; Dugas, V.; Demesmay, C.; Compagnon, I., Online Separation and Identification of Isomers Using Infrared Multiple Photon Dissociation Ion Spectroscopy Coupled to Liquid Chromatography: Application to the Analysis of Disaccharides Regio-Isomers and Monosaccharide Anomers. *Analytical Chemistry* **2018,** *90*, 11741-11745.
35. Stoll, D. R.; Carr, P. W., Two-Dimensional Liquid Chromatography: A State of the Art Tutorial. *Analytical Chemistry* **2017,** *89*, 519-531.
36. Carr, P.; Stoll, D., Two-Dimensional Liquid Chromatography—Principles, Practical Implementation and Applications. *Agilent Technologies Inc, Germany* **2015**, 182.
37. Pirok, B. W. J.; Stoll, D. R.; Schoenmakers, P. J., Recent Developments in Two-Dimensional Liquid Chromatography: Fundamental Improvements for Practical Applications. *Analytical Chemistry* **2019,** *91*, 240-263.
38. Koppen, V.; Van Looveren, C.; François, I.; Cuyckens, F., Selective drug metabolite trace analysis by very high-volume injections and heartcut two-dimensional (2D)-ultrahigh performance liquid chromatography (UHPLC). *Journal of Chromatography A* **2019,** *1601*, 164-170.
39. Martens, J.; Berden, G.; Gebhardt, C. R.; Oomens, J., Infrared ion spectroscopy in a modified quadrupole ion trap mass spectrometer at the FELIX free electron laser laboratory. *Review of Scientific Instruments* **2016,** *87*, 103108.
40. Berden, G.; Derksen, M.; Houthuijs, K. J.; Martens, J.; Oomens, J., An automatic variable laser attenuator for IRMPD spectroscopy and analysis of power-dependence in fragmentation spectra. *International Journal of Mass Spectrometry* **2019,** *443*, 1-8.
41. Pirok, B. W. J.; Gargano, A. F. G.; Schoenmakers, P. J., Optimizing separations in online comprehensive two-dimensional liquid chromatography. *Journal of Separation Science* **2018,** *41*, 68-98.
42. Prakash, C.; Shaffer, C. L.; Nedderman, A., Analytical strategies for identifying drug metabolites. *Mass Spectrometry Reviews* **2007,** *26*, 340-369.
43. Holčapek, M.; Kolářová, L.; Nobilis, M., High-performance liquid chromatography–tandem mass spectrometry in the identification and determination of phase I and phase II drug metabolites. *Analytical and Bioanalytical Chemistry* **2008,** *391*, 59-78.
44. Prasad, B.; Garg, A.; Takwani, H.; Singh, S., Metabolite identification by liquid chromatography-mass spectrometry. *TrAC Trends in Analytical Chemistry* **2011,** *30*, 360-387.
45. Outersterp, R. E. v.; Martens, J.; Berden, G.; Lubin, A.; Cuyckens, F.; Oomens, J., Identification of drug metabolites with infrared ion spectroscopy – application to midazolam *in vitro* metabolism. *ChemRxiv* **2022**.
46. Becker, S.; Kortz, L.; Helmschrodt, C.; Thiery, J.; Ceglarek, U., LC–MS-based metabolomics in the clinical laboratory. *Journal of Chromatography B* **2012,** *883-884*, 68-75.
47. Rochat, B., From targeted quantification to untargeted metabolomics: Why LC-high-resolution-MS will become a key instrument in clinical labs. *TrAC Trends in Analytical Chemistry* **2016,** *84*, 151-164.
48. Miller, M. J.; Kennedy, A. D.; Eckhart, A. D.; Burrage, L. C.; Wulff, J. E.; Miller, L. A. D.; Milburn, M. V.; Ryals, J. A.; Beaudet, A. L.; Sun, Q.; Sutton, V. R.; Elsea, S. H., Untargeted metabolomic analysis for the clinical screening of inborn errors of metabolism. *Journal of Inherited Metabolic Disease* **2015,** *38*, 1029-1039.
49. Coene, K. L. M.; Kluijtmans, L. A. J.; van der Heeft, E.; Engelke, U. F. H.; de Boer, S.; Hoegen, B.; Kwast, H. J. T.; van de Vorst, M.; Huigen, M. C. D. G.; Keularts, I. M. L. W.; Schreuder, M. F.; van Karnebeek, C. D. M.; Wortmann, S. B.;

de Vries, M. C.; Janssen, M. C. H.; Gilissen, C.; Engel, J.; Wevers, R. A., Next-generation metabolic screening: targeted and untargeted metabolomics for the diagnosis of inborn errors of metabolism in individual patients. *Journal of Inherited Metabolic Disease* **2018,** *41*, 337-353.
50. Engelke, U. F. H.; van Outersterp, R. E.; Merx, J.; van Geenen, F. A. M. G.; van Rooij, A.; Berden, G.; Huigen, M. C. D. G.; Kluijtmans, L. A. J.; Peters, T. M. A.; Al-Shekaili, H. H.; Leavitt, B. R.; de Vrieze, E.; Broekman, S.; van Wijk, E.; Tseng, L. A.; Kulkarni, P.; Rutjes, F. P. J. T.; Mecinović, J.; Struys, E. A.; Jansen, L. A.; Gospe, S. M., Jr.; Mercimek-Andrews, S.; Hyland, K.; Willemsen, M. A. A. P.; Bok, L. A.; van Karnebeek, C. D. M.; Wevers, R. A.; Boltje, T. J.; Oomens, J.; Martens, J.; Coene, K. L. M., Untargeted metabolomics and infrared ion spectroscopy identify biomarkers for pyridoxine-dependent epilepsy. *The Journal of Clinical Investigation* **2021,** *131*, e148272.
51. Crowther, L. A.-O.; Mathis, D.; Poms, M.; Plecko, B., New insights into human lysine degradation pathways with relevance to pyridoxine-dependent epilepsy due to antiquitin deficiency.
52. Struys, E. A.; Jakobs, C., Metabolism of lysine in alpha-aminoadipic semialdehyde dehydrogenase-deficient fibroblasts: evidence for an alternative pathway of pipecolic acid formation.
53. Mills, P. B.; Struys, E.; Jakobs, C.; Plecko, B.; Baxter, P.; Baumgartner, M.; Willemsen, M. A. A. P.; Omran, H.; Tacke, U.; Uhlenberg, B.; Weschke, B.; Clayton, P. T., Mutations in antiquitin in individuals with pyridoxine-dependent seizures. *Nature Medicine* **2006,** *12*, 307-309.
54. van Outersterp, R. E.; Martens, J.; Peremans, A.; Lamard, L.; Cuyckens, F.; Oomens, J.; Berden, G., Evaluation of table-top lasers for routine infrared ion spectroscopy in the analytical laboratory. *Analyst* **2021,** *146*, 7218-7229.
55. Wong, N. G. K.; Dessent, C. E. H., Illuminating the Effect of the Local Environment on the Performance of Organic Sunscreens: Insights From Laser Spectroscopy of Isolated Molecules and Complexes. *Frontiers in Chemistry* **2022,** *9*.
56. Dang, A.; Korn, J. A.; Gladden, J.; Mozzone, B.; Tureček, F., UV–Vis Photodissociation Action Spectroscopy on Thermo LTQ-XL ETD and Bruker amaZon Ion Trap Mass Spectrometers: a Practical Guide. *Journal of The American Society for Mass Spectrometry* **2019,** *30*, 1558-1564.